View metadata, citation and similar papers at core.ac.uk

brought to you by CORE

provided by University of Groningen

University of Groningen

Control of electrical networks: robustness and power sharing

Weitenberg, Erik

IMPORTANT NOTE: You are advised to consult the publisher's version (publisher's PDF) if you wish to cite from it. Please check the document version below.

Document Version
Publisher's PDF, also known as Version of record

Publication date:
2018

Link to publication in University of Groningen/UMCG research database

Citation for published version (APA):
Weitenberg, E. (2018). Control of electrical networks: robustness and power sharing. [Groningen]: Rijksuniversiteit Groningen.

Copyright
Other than for strictly personal use, it is not permitted to download or to forward/distribute the text or part of it without the consent of the author(s) and/or copyright holder(s), unless the work is under an open content license (like Creative Commons).

Take-down policy
If you believe that this document breaches copyright please contact us providing details, and we will remove access to the work immediately and investigate your claim.

Downloaded from the University of Groningen/UMCG research database (Pure): http://www.rug.nl/research/portal. For technical reasons the number of authors shown on this cover page is limited to 10 maximum.

Download date: 12-11-2019

4

Input-to-state stability with restrictions of the leaky integral controller

ABSTRACT

Frequency regulation in power systems is conventionally performed by broadcasting a centralized signal to local controllers. As a result of the energy transition, technological advances, and the scientific interest in distributed control and optimization methods, a plethora of distributed frequency control strategies have been proposed recently that rely on communication amongst local controllers. In this chapter we propose a fully decentralized leaky integral controller for frequency regulation that is derived from a classic lag element. We study steady-state, asymptotic optimality, nominal stability, input-to-state stability, noise rejection, transient performance, and robustness properties of this controller in closed loop with a nonlinear and multi-variable power system model. We demonstrate that the leaky integral controller can strike an acceptable trade-off between performance and robustness as well as between asymptotic disturbance rejection and transient convergence rate by tuning its DC gain and time constant. We compare our findings to conventional decentralized integral control and distributed-averaging-based integral control in theory and simulations.

Published as:

E. Weitenberg, Y. Jiang, C. Zhao, E. Mallada, C. De Persis, and F. Dörfler, "Robust decentralized secondary frequency control in power systems: Merits and trade-offs," *IEEE Transactions on Automatic Control*, 2017, under review.

E. Weitenberg, Y. Jiang, C. Zhao, E. Mallada, F. Dörfler, and C. De Persis, "Robust decentralized frequency control: A leaky integrator approach," in *Proceedings of the European Control Conference*, 2018.

4.1 INTRODUCTION

The core operation principle of an AC power system is to balance supply and demand in nearly real time. Any instantaneous imbalance results in a deviation of the global system frequency from its nominal value. Thus, a central control task is to regulate the frequency in an economically efficient way and despite fluctuating loads, variable generation, and possibly faults. Frequency control is conventionally performed in a hierarchical architecture: the foundation is made of the generators' rotational inertia providing an instantaneous frequency response, and three control layers – primary (droop), secondary automatic generation (AGC), and tertiary (economic dispatch) – operate at different time scales on top of it (Machowski et al., 2008; Bevrani, 2009). Conventionally, droop controllers are installed at synchronous machines and operate fully decentralized, but they cannot by themselves restore the system frequency to its nominal value. To ensure a correct steady-state frequency and a fair power sharing among generators, centralized AGC and economic dispatch schemes are employed on longer time scales.

This conventional operational strategy is currently challenged by increasing volatility on all time scales (due to variable renewable generation and increasing penetration of low-inertia sources) as well as the ever-growing complexity of power systems integrating distributed generation, demand response, microgrids, and HVDC systems, among others. Motivated by these paradigm shifts and recent advances in distributed control and optimization, an active research area has emerged developing more flexible distributed schemes to replace or complement the traditional frequency control layers.

In this chapter we focus on secondary control. We refer to Molzahn et al. (2017, Section IV.C) for a survey covering recent approaches amongst which we highlight semi-centralized broadcast-based schemes similar to AGC (Dörfler and Grammatico, 2017; Andreasson et al., 2014b; Shafiee et al., 2014) and distributed schemes relying on consensus-based averaging (Zhao et al., 2015; Dörfler et al., 2016; De Persis et al., 2016; Trip et al., 2016; Andreasson et al., 2014a; Weitenberg et al., 2017a) or primal dual methods (Li et al., 2016; Zhang and Papachristodoulou, 2015; Zhao et al., 2016; Mallada et al., 2017) that all rely on communication amongst controllers. However, due to security, robustness, and economic concerns it is desirable to regulate the frequency without relying on communication. A seemingly obvious and often advocated solution is to complement local proportional droop control with decentralized integral control (Ainsworth and Grijalva, 2013; Andreasson et al., 2014b; Zhao et al.,

2015). In theory such schemes ensure nominal and global closed-loop stability at a correct steady-state frequency, though in practice they suffer from poor robustness to measurement bias and clock drifts (Andreasson et al., 2014a,b; Dörfler and Grammatico, 2017; Schiffer et al., 2015). Furthermore, the power injections resulting from decentralized integral control generally do not lead to an efficient allocation of generation resources. A conventional remedy to overcome performance and robustness issues of integral controllers is to implement them as lag elements with finite DC gain (Franklin et al., 1994). Indeed, such decentralized lag element approaches have been investigated by practitioners: Ainsworth and Grijalva (2013) provides insights on the closed-loop steady states and transient dynamics based on numerical analysis and asymptotic arguments, Heidari et al. (2017) provides a numerical certificate for ultimate boundedness, and Han et al. (2017) analyses lead-lag filters based on a numerical small-signal analysis.

4.2 POWER SYSTEM FREQUENCY CONTROL

4.2.1 SYSTEM MODEL

Consider a lossless, connected, and network-reduced power system with n generators modelled by swing equations (Machowski et al., 2008)

$$\dot{\theta} = \omega \tag{4.1a}$$

$$M\dot{\omega} = -D\omega + P - \nabla U(\theta) + u\,, \tag{4.1b}$$

where $\theta \in \mathbb{T}^n$ and $\omega \in \mathbb{R}^n$ are the generator rotor angles and frequencies relative to the utility frequency given by $2\pi 50\,\mathrm{rad\,s^{-1}}$ or $2\pi 60\,\mathrm{rad\,s^{-1}}$. The diagonal matrices $M, D \in \mathbb{R}^{n\times n}$ collect the inertia and damping coefficients $M_i, D_i > 0$, respectively. The generator primary (droop) control is integrated in the damping coefficient D_i, $P \in \mathbb{R}^n$ is vector of nominal power injections, and $u \in \mathbb{R}^n$ is a control input to be designed later. Finally, the magnetic energy stored in the purely inductive (lossless) power transmission lines is (up to a constant) given by

$$U(\theta) = -\frac{1}{2}\sum\nolimits_{i,j=1}^{n} \mathcal{B}_{ij} V_i V_j \cos(\theta_i - \theta_j)\,,$$

where $\mathcal{B}_{ij} \geq 0$ is the susceptance of the line connecting generators i and j with terminal voltage magnitudes $V_i, V_j > 0$, which are assumed to be constant.

Observe that the vector of power injections

$$(\nabla U(\theta))_i = \sum_{j=1}^{n} \mathcal{B}_{ij} V_i V_j \sin(\theta_i - \theta_j) \tag{4.2}$$

satisfies a zero net power flow balance: $\mathbb{1}_n^\top \nabla U(\theta) = 0$, where $\mathbb{1}_n \in \mathbb{R}^n$ is the vector of unit entries. In what follows, we will also write these quantities in compact notation as

$$U(\theta) = -\mathbb{1}^\top \Gamma \cos(\mathcal{B}^\top \theta), \quad \nabla U(\theta) = \mathcal{B}\Gamma \sin(\mathcal{B}^\top \theta)\,,$$

where $\mathcal{B} \in \mathbb{R}^{n\times m}$ is the incidence matrix (Bullo, 2017) of the power transmission grid connecting the n generators with m transmission lines, and $\Gamma \in \mathbb{R}^{m\times m}$ is the diagonal matrix with its diagonal entries being all the non-zero $V_i V_j \mathcal{B}_{ij}$'s corresponding to the susceptance and voltage of the ith transmission line.

We note that all of our subsequent developments can also be extended to more detailed structure-preserving models with first-order dynamics (e.g., due to power converters), algebraic load flow equations, and variable voltages by using the techniques developed in De Persis et al. (2016); Zhao et al. (2015). In the interest of clarity, we present our ideas for the concise albeit stylized model (4.1).

4.2.2 SECONDARY FREQUENCY CONTROL

In what follows, we refer to a solution $(\theta(t), \omega(t))$ of (4.1) as a *synchronous solution* if it is of the form $\dot{\theta}(t) = \omega(t) = \omega_{\text{sync}} \mathbb{1}_n$, where ω_{sync} is the synchronous frequency.

Lemma 4.1 (Synchronization frequency)**.** *If there is a synchronous solution to the power system model* (4.1)*, then the synchronous frequency is given by*

$$\omega_{\text{sync}} = \frac{\sum_{i=1}^{n} P_i^* + \sum_{i=1}^{n} u_i^*}{\sum_{i=1}^{n} D_i}\,, \tag{4.3}$$

where u_i^* denotes the steady-state control action.

Proof. In the synchronized case, (4.1b) reduces to $D\omega_{\text{sync}}\mathbb{1}_n + \nabla U(\theta) = P + u$. After multiplying this equation by $\mathbb{1}_n^\top$ and using that $\mathbb{1}_n^\top \nabla U(\theta) = 0$, we arrive at the claim (4.3). □

Observe from (4.3) that $\omega_{\text{sync}} = 0$ if and only if all injections are balanced: $\sum_{i=1}^{n} P_i^* + u_i^* = 0$. In this case, a synchronous solution coincides with an equilibrium $(\theta^*, \omega^*, u^*) \in \mathbb{T}^n \times \{\mathbb{0}_n\} \times \mathbb{R}^n$ of (4.1). Our first objective is frequency regulation, also referred to as secondary frequency control.

Problem 4.1 (Frequency regulation)**.** Given an unknown constant vector P, design a control strategy $u = u(\omega)$ to stabilize the power system model (4.1) to an equilibrium $(\theta^*, \omega^*, u^*) \in \mathbb{T}^n \times \{\mathbb{0}_n\} \times \mathbb{R}^n$ so that $\sum_{i=1}^{n} P_i^* + u_i^* = 0$.

Observe that there are manifold choices of u^* to achieve this task. Thus, a further objective is the most economic allocation of steady-state control inputs u^* given by a solution to the following so-called *economic dispatch problem* (Wood and Wollenberg, 1996):

$$\underset{u \in \mathbb{R}^n}{\text{minimize}} \ \sum\nolimits_{i=1}^{n} a_i u_i^2 \tag{4.4a}$$

$$\text{subject to} \ \sum\nolimits_{i=1}^{n} P_i^* + \sum\nolimits_{i=1}^{n} u_i = 0 \,. \tag{4.4b}$$

The term $a_i u_i^2$ with $a_i > 0$ is the quadratic generation cost for generator i. Observe that the unique minimizer $u^\star$ of this linearly-constrained quadratic program (4.4) guarantees *identical marginal costs* at optimality (Dörfler et al., 2016; Trip et al., 2016):

$$a_i u_i^\star = a_j u_j^\star \quad \forall i, j \in \{1, \dots, n\} \,. \tag{4.5}$$

We remark that a special case of the identical marginal cost criterion (4.5) is *fair proportional power sharing* (Guerrero et al., 2011) when the coefficients a_i are chosen inversely to a reference power $\bar{P}_i > 0$ (normally the power rating) for every generator i:

$$u_i^\star / \bar{P}_i = u_j^\star / \bar{P}_j \quad \forall i, j \in \{1, \dots, n\} \,. \tag{4.6}$$

Problem 4.2 (Optimal frequency regulation)**.** Given an unknown constant vector P, design a control strategy $u = u(\omega)$ to stabilize the power system model (4.1) to an equilibrium $(\theta^*, \omega^*, u^*) \in \mathbb{T}^n \times \{\mathbb{0}_n\} \times \mathbb{R}^n$ where u^* minimizes the economic dispatch problem (4.4).

Aside from steady-state optimal frequency regulation, we will also pursue certain robustness and transient performance characteristics of the closed loop that we specify later.

4.3 FULLY DECENTRALIZED FREQUENCY CONTROL

The frequency regulation Problems 4.1 and 4.2 have seen many centralized and distributed control approaches. Since P is generally unknown, all approaches explicitly or implicitly rely on integral control of the frequency error. In the following we focus on *fully decentralized* integral control approaches making use only of local frequency measurements: $u_i = u_i(\omega_i)$.

4.3.1 DECENTRALIZED PURE INTEGRAL CONTROL

One possible control action is *decentralized pure integral control* of the locally measured frequency, that is,

$$u = -p \tag{4.7a}$$
$$T\dot{p} = \omega\,, \tag{4.7b}$$

where $p \in \mathbb{R}^n$ is an auxiliary control variable, and $T \in \mathbb{R}^{n\times n}$ is a diagonal matrix of positive time constants $T_i > 0$. The closed-loop system (4.1),(4.7) enjoys many favourable properties, such as solving the frequency regulation Problem 4.1 with *global* convergence guarantees regardless of the system or controller initial conditions or the unknown constant vector P.

Theorem 4.1 (Convergence under decentralized pure integral control)**.** *The closed-loop system* (4.1),(4.7) *has a non-empty set* $\mathcal{X}^* \subseteq \mathbb{T}^n \times \{\mathbb{0}_n\} \times \mathbb{R}^n$ *of equilibria, and all trajectories* $(\theta(t), \omega(t), p(t))$ *globally converge to* $\mathcal{X}^*$ *as* $t \to +\infty$*.*

Proof. This proof is based on an idea initially proposed in Zhao et al. (2015) while we make some arguments and derivations more rigorous here. First note that (4.7) can be explicitly integrated as

$$u = -T^{-1}(\theta - \theta_0) - p_0 = -T^{-1}(\theta - \theta_0')\,, \tag{4.8}$$

where we used $\theta_0' = \theta_0 - Tp_0$ as a shorthand. In what follows, we study only the state $(\theta(t), \omega(t))$ without $p(t)$ since $p(t)$ is a function of $\theta(t)$ and initial conditions as defined in (4.8).

Next consider the Lyapunov candidate function

$$\begin{aligned}\mathcal{V}(\theta,\omega) = &\frac{1}{2}\omega^\top M\omega + U(\theta) - \theta^\top P\\ &+ \frac{1}{2}(\theta - \theta_0')^\top T^{-1}(\theta - \theta_0')\end{aligned} \tag{4.9}$$

The derivative of $\mathcal{V}$ along any trajectory of (4.1), (4.7) is

$$\dot{\mathcal{V}}(\theta, \omega) = -\omega^\top D \omega \,. \tag{4.10}$$

Note that for any initial condition $(\theta_0, \omega_0) \in \mathbb{T}^n \times \mathbb{R}^n$ the sublevel set $\Omega := \{(\theta, \omega) \mid \mathcal{V}(\theta, \omega) \leq \mathcal{V}(\theta_0, \omega_0)\}$ is compact. Indeed Ω is closed due to continuity of $\mathcal{V}$ and bounded since $\mathcal{V}$ is radially unbounded due to quadratic terms in ω and θ. The set Ω is also forward invariant since $\dot{\mathcal{V}} \leq 0$ by (4.10).

In order to proceed, define the zero-dissipation set

$$\mathcal{E} = \left\{(\theta, \omega) \mid \dot{\mathcal{V}}(\theta, \omega) = 0\right\} = \{(\theta, \omega) \mid \omega = \mathbb{0}_n\} \tag{4.11}$$

and $\mathcal{E}_\Omega := \mathcal{E} \cap \Omega$. By LaSalle's theorem (Khalil, 2002, Theorem 4.4), as $t \to +\infty$, $(\theta(t), \omega(t))$ converges to a non-empty, compact, invariant set $\mathcal{L}_\Omega$ which is a subset of $\mathcal{E}_\Omega$. In the following, we show that any point $(\theta', \omega') \in \mathcal{L}_\Omega$ is an equilibrium of (4.1),(4.7). Due to the invariance of $\mathcal{L}_\Omega$, the trajectory $(\theta(t), \omega(t))$ starting from (θ', ω') stays identically in $\mathcal{L}_\Omega$ and thus in $\mathcal{E}_\Omega$. Therefore, by (4.11) we have $\omega(t) \equiv 0$ and hence $\dot{\omega}(t) \equiv 0$. Thus, every point on this trajectory, in particular the starting point (θ', ω'), is an equilibrium of (4.1),(4.7). This completes the proof. □

The global convergence merit of decentralized integral control comes at a cost though. First, note that the steady-state injections from decentralized integral control (4.7),

$$u^* = -T^{-1}(\theta^* - \theta_0) - p_0,$$

depend on initial conditions and the unknown values of P. Thus, in general u^* does not meet the optimality criterion (4.5). Second and more importantly, *internal instability* due to decentralized integrators is a known phenomenon in control systems (Campo and Morari, 1994; Åström and Hägglund, 2006). In our particular scenario, as shown in Andreasson et al. (2014a, Theorem 1) and Dörfler and Grammatico (2017, Proposition 1), the decentralized integral controller (4.7) is not robust to arbitrarily small biased measurement errors that may arise, e.g., due to clock drifts (Schiffer et al., 2015). More precisely the closed-loop system consisting of (4.1) and the integral controller subject to measurement bias $\eta \in \mathbb{R}^n$

$$u = -p \tag{4.12a}$$
$$T\dot{p} = \omega + \eta \,, \tag{4.12b}$$

does not admit any synchronous solution unless $\eta \in \operatorname{span}(\mathbb{1}_n)$, that is, all biases η_i, for all $i \in \{1, \dots, n\}$, are perfectly identical (Dörfler and Grammatico, 2017, Proposition 1). Thus, while theoretically favourable, the decentralized integral controller (4.7) is not practical.

4.3.2 DECENTRALIZED LAG AND LEAKY INTEGRAL CONTROL

In standard frequency-domain control design (Franklin et al., 1994) a stable and finite DC-gain implementation of a proportional-integral (PI) controller is given by a *lag element* parametrized as

$$\alpha \frac{Ts+1}{\alpha Ts+1} = \underbrace{1}_{\text{proportional control}} + \underbrace{\frac{\alpha-1}{\alpha Ts+1}}_{\text{leaky integral control}},$$

where $T > 0$ and $\alpha \gg 1$. The lag element consists of a proportional channel as well as a first-order lag often referred to as a *leaky integrator*. In our context, a state-space realization of a decentralized lag element for frequency control is

$$\begin{aligned} u &= -\omega - (\alpha-1)p \\ \alpha T\dot{p} &= \omega - p\,, \end{aligned}$$

where T is a diagonal matrix of time constants, and $\alpha \gg 1$ is scalar. In what follows we disregard the proportional channel (that would add further droop) and focus on the leaky integrator to remedy the shortcomings of pure integral control (4.7).

Consider the *leaky integral controller*

$$u = -p \tag{4.13a}$$
$$T\dot{p} = \omega - Kp\,, \tag{4.13b}$$

where $K, T \in \mathbb{R}^{n\times n}$ are diagonal matrices of positive control gains $K_i, T_i > 0$. The transfer function of the leaky integral controller (4.13) at a node i (from ω_i to $-u_i$) given by

$$\mathcal{K}_i(s) = \frac{1}{T_i s + K_i} = \frac{K_i^{-1}}{(T_i/K_i)\cdot s + 1}\,, \tag{4.14}$$

i.e., the leaky integrator is a first-order lag with *DC gain* K_i^{-1} and *time constant* T_i/K_i (which also equals the bandwidth). It is instructive to consider the limiting values for the gains:

1. For $T_i \searrow 0$, leaky integral control (4.13) reduces to proportional (droop) control with gain K_i^{-1};
2. for $K_i \searrow 0$, we recover the pure integral control (4.7);
3. and for $K_i \nearrow \infty$ or $T_i \nearrow \infty$, we obtain an open-loop system without control action.

Thus, from loop-shaping perspective for open-loop stable SISO systems, we expect good steady-state frequency regulation for a large DC gain K_i^{-1}, and a large (respectively, small) cut-off frequency K_i/T_i likely results in good nominal transient performance (respectively, good noise rejection). We will confirm these intuitions in the next section, where we analyse the leaky integrator (4.13) in closed loop with the nonlinear and multi-variable power system (4.1) and highlight its merits and trade-offs as function of the gains K and T.

4.4 PROPERTIES OF THE LEAKY INTEGRAL CONTROLLER

The power system model (4.1) controlled by the leaky integrator (4.13) gives rise to the closed-loop system

$$\dot{\theta} = \omega \tag{4.15a}$$
$$M\dot{\omega} = -D\omega + P - \nabla U(\theta) - p \tag{4.15b}$$
$$T\dot{p} = \omega - Kp\,. \tag{4.15c}$$

We make the following standing assumption on this system.

Assumption 4.1 (Existence of a synchronous solution)**.** *Assume that the closed-loop* (4.15) *admits a synchronous solution* $(\theta^*, \omega^*, p^*)$ *of the form*

$$\dot{\theta}^* = \omega^* \tag{4.16a}$$
$$\mathbb{0}_n = -D\omega^* + P - \nabla U(\theta^*) - p^* \tag{4.16b}$$
$$\mathbb{0}_n = \omega^* - Kp^*\,. \tag{4.16c}$$

where $\omega^* = \omega_{\text{sync}}\mathbb{1}_n$ *for some* $\omega_{\text{sync}} \in \mathbb{R}$.

By eliminating the variable p^* from (4.16), we arrive at

$$P - (D + K^{-1})\,\omega_{\text{sync}}\mathbb{1}_n = \nabla U(\theta^*)\,. \tag{4.17}$$

Equations (4.17) take the form of lossless active power flow equations (Machowski et al., 2008) with injections $P - (D + K^{-1})\,\omega_{\text{sync}}\mathbb{1}_n$. Thus, Assumption 4.1 is equivalent assuming feasibility of the power flow (4.17) which is always true for sufficiently small $\|P\|$.

Under this assumption, we now show various properties of the closed-loop system (4.15) under leaky integral control (4.13).

4.4.1 STEADY-STATE ANALYSIS

We begin our analysis by studying the steady-state characteristics. At steady state, the control input u^* takes the value

$$u^* = -P = -K^{-1}\omega^* = -K^{-1}\omega_{\text{sync}}\mathbb{1}_n\,, \tag{4.18}$$

that is, it has a finite DC gain K^{-1} similar to a primary droop control. The following result is analogous to Lemma 4.1.

Lemma 4.2 (Steady-state frequency)**.** *Consider the closed-loop system* (4.15) *and its equilibria* (4.16)*. The explicit synchronization frequency is given by*

$$\omega_{\text{sync}} = \frac{\sum_{i=1}^n P_i^*}{\sum_{i=1}^n D_i + K_i^{-1}} \tag{4.19}$$

Unsurprisingly, the leaky integral controller (4.13) does generally not regulate the synchronous frequency ω_{sync} to zero unless $\sum_i P_i^* = 0$. However, it can achieve *approximate frequency* regulation within a pre-specified tolerance band.

Corollary 4.1 (Banded frequency regulation)**.** *Consider the closed-loop system* (4.15)*. The synchronous frequency ω_{sync} takes value in a band around zero that can be made arbitrarily small by choosing the gains $K_i > 0$ sufficiently small. In particular, for any $\epsilon > 0$, if*

$$\sum\nolimits_{i=1}^n K_i^{-1} \geq \frac{\left|\sum_{i=1}^n P_i^*\right|}{\epsilon} - \sum\nolimits_{i=1}^n D_i\,,$$

then $|\omega_{\text{sync}}| \leq \epsilon$.

While regulating the frequencies to a narrow band is sufficient in practical applications, the closed-loop performance may suffer since the control input (4.13) may become ineffective due to a small bandwidth K_i/T_i. Similar observations have also been made in Ainsworth and Grijalva (2013); Heidari et al.

(2017). We will repeatedly encounter this trade-off for the decentralized leaky integral controller (4.13) between choosing a small gain K (for desirable steady-state properties) and large gain (for transient performance).

The closed-loop steady-state injections are given by (4.18), and we conclude that the leaky integral controller achieves proportional power sharing by tuning its gains appropriately:

Corollary 4.2 (Steady-state power sharing)**.** *Consider the closed-loop system* (4.15)*. The steady-state injections u^* of the leaky integral controller achieve fair proportional power sharing as follows:*

$$K_i u_i^* = K_j u_j^* \quad \forall i, j \in \{1, \dots, n\} \,. \tag{4.20}$$

Hence, arbitrary power sharing ratios as in (4.6) can be prescribed by choosing the control gains as $K_i \sim 1/\bar{P}_i$. Similarly, we have the following result on steady-state optimality:

Corollary 4.3 (Steady-state optimality)**.** *Consider the closed-loop system* (4.15)*. The steady-state injections u^* of the leaky integral controller minimize the economic dispatch problem*

$$\underset{u \in \mathbb{R}^n}{\text{minimize}} \ \sum\nolimits_{i=1}^{n} K_i u_i^2 \tag{4.21a}$$

$$\text{subject to} \ \sum_{i=1}^{n} P_i^* + \sum_{i=1}^{n} (1 + D_i K_i) u_i = 0 \,. \tag{4.21b}$$

Proof. Observe from (4.20) that the steady-state injections (4.18) meet the identical marginal cost requirement (4.5) with $a_i = K_i$. Additionally, the steady-state equations (4.16b), (4.16c), and (4.18) can be merged to the expression

$$\mathbb{0}_n = DK u^* + P - \nabla U(\theta^*) + u^* \,.$$

By multiplying this equation from the left by $\mathbb{1}_n^\top$, we arrive at the condition (4.21b). Hence, the injections u^* are also feasible for (4.21) and thus optimal for the program (4.21). □

The steady-state injections of the leaky integrator are optimal for the modified dispatch problem (4.21) with appropriately chosen cost functions. By (4.21b), the leaky integrator does not achieve perfect power balancing $\sum_{i=1}^{n} P_i^* + u_i^* = 0$ and underestimates the net load, but it can satisfy the power balance (4.4b) arbitrarily well for K chosen sufficiently small.

4.4.2 STABILITY & ROBUSTNESS ANALYSIS

For ease of analysis, in this subsection we introduce a change of coordinates for the voltage phase angle θ. Let $\delta = \theta - \frac{1}{n}\mathbb{1}_n\mathbb{1}_n^\top\theta = \Pi\theta$ be the centre-of-inertia coordinates (see e.g. Sauer and Pai, 1998; De Persis et al., 2016), where $\Pi = I - \frac{1}{n}\mathbb{1}_n\mathbb{1}_n^\top$. In these coordinates, the open-loop system (4.1) becomes

$$\dot{\delta} = \Pi\omega \tag{4.22a}$$

$$M\dot{\omega} = -D\omega + P - \nabla U(\delta) + u, \tag{4.22b}$$

where by an abuse of notation we use the same symbol U for the potential function expressed in terms of δ,

$$U(\delta) = -\mathbb{1}^\top\Gamma\cos(\mathcal{B}^\top\delta), \quad \nabla U(\delta) = \mathcal{B}\Gamma\sin(\mathcal{B}^\top\delta).$$

Note that $\mathcal{B}^\top\Pi = \mathcal{B}^\top$ since $\mathcal{B}^\top\mathbb{1}_n = \mathbb{0}_n$ (Bullo, 2017). The synchronous solution $(\theta^*, \omega^*, p^*)$[1] defined in (4.16) is mapped into the point $(\delta^*, \omega^*, p^*)$, with $\delta^* = \Pi\theta^*$, satisfying

$$\dot{\delta}^* = \mathbb{0}_n \tag{4.23a}$$

$$\mathbb{0}_n = -D\omega^* + P - \nabla U(\delta^*) - P \tag{4.23b}$$

$$\mathbb{0}_n = \omega^* - KP. \tag{4.23c}$$

The existence of $(\delta^*, \omega^*, p^*)$ is guaranteed by Assumption 4.1. Additionally, we make the following standard assumption constraining steady-state angle differences.

Assumption 4.2 (Security constraint)**.** *The synchronous solution* (4.23) *is such that* $\mathcal{B}^\top\delta^* \in \Theta := (-\frac{\pi}{2} + \rho, \frac{\pi}{2} - \rho)^m$ *for a constant scalar* $\rho \in \left(0, \ \frac{\pi}{2}\right)$.

Remark 4.1. Compared with the conventional security constraint assumption (Dörfler et al., 2016), we introduce an extra margin ρ on the constraint to be able to explicitly quantify the decay of the Lyapunov function we use in proofs of Theorems 4.2 and 4.3.

By using Lyapunov techniques following Weitenberg et al. (2017a), it is possible to show that the leaky integral controller (4.13) guarantees exponential stability of the synchronous solution (4.23).

[1] Of course, care must be taken when interpreting the results in this section since the steady-state itself depends on the controller gain K (see Section 4.4.1). Here we are merely interested in the stability relative to the equilibrium.

Theorem 4.2 (Exponential stability under leaky integral control)**.** *Consider the closed-loop system* (4.22), (4.13)*. Let Assumptions 4.1 and 4.2 hold. The equilibrium* $(\delta^*, \omega^*, p^*)$ *is locally exponentially stable. In particular, given the incremental state*

$$x = x(\delta, \omega, p) = \mathrm{col}(\delta - \delta^*, \omega - \omega^*, p - p^*), \tag{4.24}$$

the solutions $x(t) = \mathrm{col}(\delta(t) - \delta^*, \omega(t) - \omega^*, p(t) - p^*)$*, with* $(\delta(t), \omega(t), p(t))$ *a solution to* (4.22), (4.13) *that start sufficiently close to the origin satisfy for all* $t \geq 0$*,*

$$\|x(t)\|^2 \leq \lambda e^{-\alpha t} \|x_0\|^2, \tag{4.25}$$

where λ *and* α *are positive constants. In particular, when multiplying the gains K and T by the positive scalars* κ *and* τ *respectively,* α *is monotonically non-decreasing as a function of the gain* κ *and non-increasing as a function of* τ*.*

Proof. Consider the incremental Lyapunov function from Weitenberg et al. (2017a) including a cross-term between potential and kinetic energy:

$$\begin{aligned} V(x) = &\frac{1}{2}(\omega - \omega^*)^\top M(\omega - \omega^*) \\ &+ U(\delta) - U(\delta^*) - \nabla U(\delta^*)^\top(\delta - \delta^*) \\ &+ \frac{1}{2}(p - P)^\top T(p - P) \\ &+ \varepsilon(\nabla U(\delta) - \nabla U(\delta^*))^\top M\omega\,, \end{aligned} \tag{4.26}$$

where $\varepsilon \in \mathbb{R}$ is a small positive parameter. For sufficiently small values of ε and if Assumption 4.2 holds, $V(x)$ satisfies

$$\beta_1 \|x\|^2 \leq V(x) \leq \beta_2 \|x\|^2 \tag{4.27}$$

for some $\beta_1, \beta_2 > 0$ and for all x with $\mathcal{B}^\top \delta \in \Theta$, by Lemma 4.3 in Appendix 4.7. The derivative of $V(x)$ can be expressed as

$$\dot{V}(x) = -\chi^\top H(\delta)\chi,$$

where $\chi(\delta, \omega, p) := \mathrm{col}(\nabla U(\delta) - \nabla U(\delta^*), \omega - \omega^*, p - p^*)$,

$$H(\delta) = \begin{bmatrix} \varepsilon I & \frac{1}{2}\varepsilon D & -\frac{1}{2}\varepsilon I \\ \frac{1}{2}\varepsilon D & D - \varepsilon E(\delta) & \mathbb{0}_{n\times n} \\ -\frac{1}{2}\varepsilon I & \mathbb{0}_{n\times n} & K \end{bmatrix}, \tag{4.28}$$

and we defined the shorthand $E(\delta) = \mathrm{sp}(M\nabla^2 U(\delta))$ with $\mathrm{sp}(A) = \frac{1}{2}(A + A^\top)$. We claim that for all δ, $H(\delta) > 0$. To see this, apply Lemma 2.5 from Appendix 4.7 to obtain $H(\delta) \geq H'(\delta)$ with

$$H'(\delta) := \begin{bmatrix} \frac{\varepsilon}{2} I & \mathbb{0}_{n\times n} & \mathbb{0}_{n\times n} \\ \mathbb{0}_{n\times n} & D - \varepsilon(E(\delta) + D^2) & \mathbb{0}_{n\times n} \\ \mathbb{0}_{n\times n} & \mathbb{0}_{n\times n} & K - \varepsilon I \end{bmatrix}.$$

Given that D and K are positive definite matrices, one can select ε to be positive yet sufficiently small so that $H'(\delta) > 0$.

Additionally, we claim that a positive constant β_3, dependent on ρ from Assumption 4.2, exists such that $\|\chi\|^2 \geq \beta_3 \|x\|^2$. To see this, we note that from Lemma 2.4 that a constant β_3' exists so that

$$\|\nabla U(\delta) - \nabla U(\bar{\delta})\|^2 \leq \beta_3' \|\delta - \delta^*\|^2. \tag{4.29}$$

The claim then follows with $\beta_3 = \min(1, {\beta_3'}^{-1})$.

In order to proceed, we set $\beta_4 := \min_{\mathcal{B}^\top \delta \in \Theta} \lambda_{\min}(H(\delta))$. Then, it follows using (4.27) that, as far as $\mathcal{B}^\top \delta \in \Theta$,

$$\dot{V}(x) \leq -\beta_4 \|\chi\|^2 \leq -\beta_3 \beta_4 \|x\|^2 \leq -\frac{\beta_3 \beta_4}{\beta_2} V =: -\alpha V(x)\,.$$

For this inequality to lead to the claimed exponential stability, we must guarantee that the solutions do not leave Θ. Recall that the sublevel sets of $V(x)$ are invariant and thus solutions $x(t)$ are bounded for all $t \geq 0$ in sublevel sets $\{x : V(x) \leq V(x_0)\}$ for which $\mathcal{B}^\top \delta \in \Theta$. Hence, we require the initial conditions x_0 of solutions $x(t)$ to be within a suitable sublevel set $\{x : V(x) \leq V(x_0)\}$ where $\mathcal{B}^\top \delta \in \Theta$. We now construct such a sublevel set. Let

$$c := \beta_1 \frac{\xi^2}{\lambda_{\max}(\mathcal{B}\mathcal{B}^\top)} \tag{4.30}$$

and $\xi > 0$ a parameter with the property that any δ satisfying $\|\mathcal{B}^\top \delta - \mathcal{B}^\top \delta^*\| \leq \xi$ also satisfies $\mathcal{B}^\top \delta \in \Theta$. The parameter ξ exists because $\mathcal{B}^\top \delta^* \in \Theta$ and Θ is an open set. Accordingly, define the sublevel set $\Omega_c := \{x : V(x) \leq c\}$, with c defined above, and note that any point in Ω_c satisfies $\mathcal{B}^\top \delta \in \Theta$. As a matter of fact $V(x) \leq c$ implies $\|x\|^2 \leq \frac{\xi^2}{\lambda_{\max}(\mathcal{B}\mathcal{B}^\top)}$ and therefore $\|\delta - \delta^*\|^2 \leq \frac{\xi^2}{\lambda_{\max}(\mathcal{B}\mathcal{B}^\top)}$.

This in turn implies that $\|\mathcal{B}^\top(\delta-\delta^*)\|^2 \leq \xi^2$, and hence $\mathcal{B}^\top\delta \in \Theta$ by the choice of ξ.

We conclude that any solution issuing from the sublevel set Ω_c will remain inside of it. Hence along these solutions the inequality $\dot{V}(x) \leq -\alpha V(x)$ holds for all time.

By the comparison lemma (Khalil, 2014, Lemma B.2), this inequality yields $V(x(t)) \leq e^{-\alpha t}V(x(0))$, which we combine again with (4.27) to arrive at (4.25) with $\lambda = \beta_2/\beta_1$.

Finally, we address the effect of K and T on α by introducing the scalar factors κ and τ multiplying K and T. Note that α is a monotonically increasing function of $\beta_4 = \min_{\mathcal{B}^\top\delta\in\Theta}\lambda_{\min}(H(\delta))$. Recall that for any vector z,

$$\lambda_{\min}(H(\delta))\|z\|^2 \leq z^\top H(\delta)z,$$

with equality if z is the eigenvector corresponding to $\lambda_{\min}(H(\delta))$. Let $e_{\min}$ denote the normalized eigenvector corresponding to $\lambda_{\min}(H(\delta))$. Then, for any vector z satisfying $\|z\| = 1$, $\lambda_{\min}(H(\delta)) = e_{\min}^\top H(\delta)e_{\min} \leq z^\top H(\delta)z$. Hence,

$$\beta_4 = \min_{\mathcal{B}^\top\delta\in\Theta}\lambda_{\min}(H(\delta)) = \min_{\mathcal{B}^\top\delta\in\Theta\,,\,z:\|z\|=1} z^\top H(\delta)z,$$

where the last equality holds by noting that $e_{\min}$ is one of the vectors z at which the minimum is attained.

Now suppose we multiply K by a factor $\kappa > 1$. Let

$$H'(\delta) = H(\delta) + \operatorname{block\,diag}(\mathbb{0},\mathbb{0},(\kappa-1)K).$$

The new value of β_4 is

$$\beta_4' = \min_{\mathcal{B}^\top\delta\in\Theta\,,\,z:\|z\|=1} \underbrace{\left(z^\top H(\delta)z + \sum\nolimits_{i=1}^{n}(\kappa-1)K_i z_{2n+i}^2\right)}_{=z^\top H'(\delta)z}.$$

The argument of the minimization is not smaller than $z^\top H(\delta)z$ for any z. It follows that $\beta_4' \geq \min_{\mathcal{B}^\top\delta\in\Theta\,,\,z:\|z\|=1} z^\top H(\delta)z = \beta_4$. Similarly, if $0 < \kappa < 1$, then $\beta_4' \leq \min_{\mathcal{B}^\top\delta\in\Theta\,,\,z:\|z\|=1} z^\top H(\delta)z = \beta_4$. Hence, β_4 is a monotonically non-decreasing function of the gain κ. Likewise, α is a monotonically decreasing function of β_2, which itself is a non-decreasing function of τ. □

Theorem 4.2 is in line with the loop-shaping insight that the bandwidth K_i/T_i determines nominal performance, that is, the decay rate α is monotonically non-decreasing in K_i/T_i.

We now depart from nominal performance and focus on robustness. Recall a key disadvantage of pure integral control: it is not robust to biased measurement errors of the form (4.12). We now show that leaky integral control (4.13) is robust to such measurement errors. In what follows, instead of (4.13), consider leaky integral control subjected to measurement errors

$$u = -p \tag{4.31a}$$
$$T\dot{p} = \omega - Kp + \eta\,, \tag{4.31b}$$

where the measurement noise $\eta = \eta(t) \in \mathbb{R}^n$ is assumed to be an ∞-norm bounded disturbance. In this case, the bias-induced instability (reported in Section 4.3.1) does not occur.

Let us first offer a qualitative steady-state analysis. For a constant vector η, the equilibrium equation (4.16c) becomes

$$\mathbb{0}_n = \omega^* - KP + \eta.$$

so that the closed loop (4.1), (4.31) will admit synchronous equilibria. Indeed, the governing equations (4.17) determining the synchronous frequency ω_{sync} change to

$$(D + K^{-1})\,\omega_{\text{sync}}\mathbb{1} = P - \nabla U(\theta^*) - K^{-1}\eta\,.$$

Observe that the noise terms η now takes the same role as the constant injections P, and their effect can be made arbitrarily small by increasing K. We now make this qualitative steady-state reasoning more precise and derive a robustness criterion by means of the same Lyapunov approach used to prove Theorem 4.2. We take the measurement error η as disturbance input and quantify its effect on the convergence behaviour along the lines of input-to-state stability. First, we define the specific robust stability criterion that we will use, repeating Definition 3.1.

Definition 4.1. A system $\dot{x} = f(x, \eta)$ is said to be input-to-state stable (ISS) with restriction $\mathcal{X}$ on $x(0) = x_0$ and restriction $\overline{\eta} \in \mathbb{R}_{>0}$ on $\eta(\cdot)$ if there exist a class $\mathcal{KL}$-function β and a class $\mathcal{K}_\infty$-function γ such that for all $t \in \mathbb{R}_{\geq 0}$, $x_0 \in \mathcal{X}$, and all $\eta(\cdot) \in L^n_\infty$ satisfying

$$\|\eta(\cdot)\|_\infty := \operatorname*{ess\,sup}_{t \in \mathbb{R}_{\geq 0}} \|\eta(t)\| \leq \overline{\eta},$$

we have

$$\|x(t)\| \leq \beta(\|x_0\|, t) + \gamma(\|\eta(\cdot)\|_\infty).$$

Theorem 4.3 (ISS under biased leaky integral control)**.** *Consider system* (4.22) *in closed-loop with the biased leaky integral controller* (4.31)*. Let Assumptions 4.1 and 4.2 hold. Given a diagonal matrix $K > 0$, there exist a positive constant $\overline{\eta}$ and a set $\mathcal{X}$ such that the closed-loop system is ISS from the noise η to the state $x = \mathrm{col}(\delta - \delta^*, \omega - \omega^*, p - p^*)$ with restrictions $\mathcal{X}$ on x_0 and $\overline{\eta}$ on $\eta(\cdot)$, where (δ^*, ω^*, P) is the equilibrium of the nominal system, i.e., with $\eta = 0$. In particular, the solutions $x(t) = \mathrm{col}(\delta(t) - \delta^*, \omega(t) - \omega^*, p(t) - p^*)$, with $(\delta(t), \omega(t), p(t))$ a solution to* (4.22)*,* (4.31) *for which $x(0) \in \mathcal{X}$ and $\|\eta(\cdot)\|_\infty \leq \overline{\eta}$ satisfy for all $t \in \mathbb{R}_{\geq 0}$,*

$$\|x(t)\|^2 \leq \lambda e^{-\hat{\alpha}t}\|x(0)\|^2 + \gamma\|\eta(\cdot)\|_\infty^2, \tag{4.32}$$

where $\hat{\alpha}$, λ and γ are positive constants. Furthermore, when multiplying the gains K and T by the positive scalars κ and τ respectively, then γ is monotonically decreasing (respectively, non-increasing) as a function of κ (respectively, τ), and $\hat{\alpha}$ is monotonically non-decreasing as a function of κ and non-increasing as a function of τ.

Proof. From the proof of Theorem 4.2 recall the Lyapunov function derivative $\dot{V}(x) = -\chi^\top H(\delta)\chi - (p - P)^\top \eta$. Since for any positive parameter μ,

$$-(p - P)^\top \eta \leq \mu\|p - P\|^2 + \frac{1}{\mu}\|\eta\|^2,$$

one further obtains

$$\dot{V}(x) \leq -\chi^\top \underbrace{\left(H(\delta) - \begin{bmatrix} \mathbb{0} & \mathbb{0} & \mathbb{0} \\ \mathbb{0} & \mathbb{0} & \mathbb{0} \\ \mathbb{0} & \mathbb{0} & \mu I \end{bmatrix}\right)}_{=\hat{H}(\delta)} \chi + \frac{1}{\mu}\|\eta\|^2.$$

Following the reasoning in the proof of Theorem 4.2, we note that $\hat{H}(\delta) \geq \hat{H}'(\delta)$, where

$$\hat{H}'(\delta) := \begin{bmatrix} \frac{\varepsilon}{2} I & \mathbb{0}_{n\times n} & \mathbb{0}_{n\times n} \\ \mathbb{0}_{n\times n} & D - \varepsilon(E(\delta) + D^2) & \mathbb{0}_{n\times n} \\ \mathbb{0}_{n\times n} & \mathbb{0}_{n\times n} & K - \varepsilon I - \mu I \end{bmatrix}.$$

It follows that for sufficiently small values of ε and μ, $\hat{H}(\delta) \geq \hat{H}'(\delta) > 0$. To continue, let $\hat{\beta}_4 := \min_{\mathcal{B}^\top \delta \in \Theta} \lambda_{\min}(\hat{H}(\delta))$. As a result, we find that for a positive constant $\hat{\alpha} = \frac{\beta_3 \hat{\beta}_4}{\beta_2}$,

$$\dot{V}(x) \leq -\hat{\alpha}V(x) + \frac{1}{\mu}\|\eta\|^2 \tag{4.33}$$

for all x such that $\mathcal{B}^\top \delta \in \Theta$. In the remainder of the proof, we fix $\bar{\eta}$ such that

$$\bar{\eta} = \hat{\alpha} c \mu.$$

with c defined as in (4.30) in the proof of Theorem 4.2.

Define the sublevel set Ω_c, again as in the proof of Theorem 4.2. We now claim that the solutions of the closed-loop system cannot leave Ω_c. In fact, on the boundary $\partial\Omega_c$ of the sublevel set Ω_c, the right-hand side of (4.33) equals $-\hat{\alpha}c + \frac{1}{\mu}\|\eta\|^2$, which is a non-positive constant by the choice of $\bar{\eta}$. Hence a solution leaving Ω_c would contradict the property that $\dot{V}(x) \leq 0$ for all $x \in \partial\Omega_c$. We conclude that all solutions must satisfy (4.33) for all $t \in \mathbb{R}_{\geq 0}$. Hence, we choose $\mathcal{X} = \Omega_c$.

By applying the Comparison Lemma, the use of a convolution integral and bounding $\|\eta(t)\|^2$ by $\|\eta(\cdot)\|_\infty^2$, we arrive at

$$V(x(t)) \leq e^{-\hat{\alpha}t} V(x_0) + \frac{1}{\hat{\alpha}\mu} \|\eta(\cdot)\|_\infty^2.$$

We combine this inequality with (4.27) and (4.29) to arrive at (4.32) with $\lambda = \beta_2/\beta_1$ and $\gamma = (\hat{\alpha}\beta_1\mu)^{-1}$.

Finally, we address the effect of K and T on $\hat{\alpha}$ and γ by introducing the scalar factors κ and τ multiplying K and T.

As κ increases, there is no need to increase ε, while it is possible to increase μ. Analogously to the reasoning in the proof of Theorem 4.2, increasing the value of κ for constant ε and increasing μ can not lower the value of $\hat{\beta}_4$ and $\hat{\alpha}$, and decreases the value of γ. If one *decreases* κ, but multiplies μ by the same factor so as to keep $\hat{\beta}_4$ constant, μ will also decrease. This guarantees $\hat{\alpha}$ remains constant in this case, preserving its status as a non-decreasing function of κ. On the other hand, a decrease in μ results in an increase in γ, retaining its status as a decreasing function of κ. Therefore, $\hat{\alpha}$ is non-decreasing as a function of κ and γ is decreasing.

As in Theorem 4.2, τ affects only β_1 and β_2, and the same result holds: $\hat{\alpha}$ is a monotonically non-increasing function of τ. Analogously, γ is monotonically non-increasing in τ. □

Theorem 4.3 shows that larger gains K (and T) reduce (respectively, do not amplify) the effect of the noise η on the state x. This further emphasizes the trade-off between frequency banding and controller performance already noted

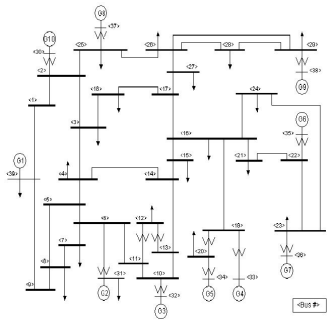

Figure 4.1: The 39-bus New England system used in simulations.

in Section 4.4.1. The intuition that a large gain T is beneficial (more precisely not detrimental) for noise rejection was expected from a loop-shaping perspective. Theorem 4.3 extends these observations to the dynamic response of the nonlinear and multi-variable closed-loop system. Notice, however, that K affects the safety region as well as the equilibrium of the system and should be selected carefully.

Remark 4.2 (Exponential ISS with restrictions)**.** The $\mathcal{KL}$–function from the ISS inequality (4.32) is an exponential function, so the stability property is in fact exponential ISS with restrictions. The need to include restrictions $\mathcal{X}$ on the initial conditions and $\bar{\eta}$ on the noise is due to the requirement of maintaining the state response within the safety region Θ.

4.5 CASE STUDY: IEEE 39 NEW ENGLAND SYSTEM

In this section we perform a case study with the 39-bus New England system, see Figure 4.1, which is modelled as in (4.1)-(4.2) with parameters M_i (for the 10 generator buses), V_i, and $\mathcal{B}_{ij}$ taken from Chow et al. (2000). The inertia coefficients M_i are set to zero for the 29 (load) buses without generators. For every generator bus i, the damping coefficient D_i is chosen as 20 per unit (pu) so that a 0.05 pu (3 Hz) change in frequency will cause a 1 pu (1000 MW) change in the generator output power. For every load bus i, D_i is chosen as $1/200$ of that of a generator. For all simulations below, a 300 MW step increase in active-power load occurs at each of buses 15, 23, 39 at time $t = 5\,\mathrm{s}$.

4.5.1 COMPARISON BETWEEN CONTROLLERS WITHOUT NOISE

We implement each of the following controllers across the 10 generators to stabilize the system after the increase in load:

1. *distributed-averaging based integral control* (DAI):

$$u = -p \tag{4.34a}$$
$$T\dot{p} = A^{-1}\omega - LAp\,. \tag{4.34b}$$

   Here $L = L^\top$ is the Laplacian matrix of a communication graph among the controllers, which we choose as a ring graph with uniform weights 0.1. The matrix A is diagonal with entries $A_{ii} = a_i$ being the cost coefficients in (4.4a) chosen as 1.0 for generators G3, G5, G6, G9, G10 and 2.0 for all others. We choose the time constant $T_i = 0.05\,\mathrm{s}$ for every generator i. The DAI control (4.34) is known to achieve stable and optimal frequency regulation as in Problem 4.2; see Zhao et al. (2015); Dörfler et al. (2016); De Persis et al. (2016); Trip et al. (2016); Andreasson et al. (2014a); Weitenberg et al. (2017a). Even DAI control is based on a reliable and fast communication environment, we include it here as a baseline for comparison purposes.

2. *decentralized pure integral control* (4.7) with time constant $T_i = 0.05\,\mathrm{s}$ for every generator i.

3. *decentralized leaky integral control* (4.13) with time constant $T_i = 0.05\,\mathrm{s}$ for every generator i. The gain K_i equals 0.005 for generators G3, G5, G6, G9, G10 and 0.01 for the others. The K_i's are proportional to a_i's in DAI (4.34) so that the dispatch objectives (4.4a) and (4.21a) are identical.

Figure 4.2 (dashed plots) shows the frequency at G1 (all other generators display similar frequency trends), and Figure 4.3 shows the active-power outputs of all generators, under the different controllers above and without noisy measurements. First, note that all closed-loop systems reach stable steady-states; see Theorems 4.1 and 4.3. Second, observe from Figure 4.2 that both pure integral and DAI control can perfectly restore the frequencies to the nominal value, whereas leaky integral control leads to a steady-state frequency error as predicted in Lemma 4.2. Third, as observed from Figure 4.3, both DAI and leaky integral control achieve the desired asymptotic power sharing (2:1

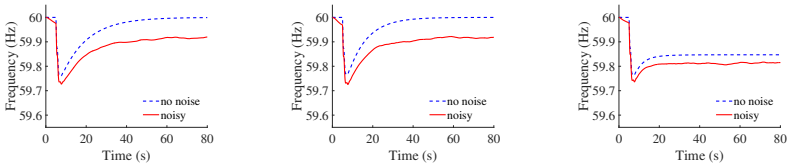

(a) DAI control (b) Decentralized pure integral control (c) Leaky integral control

Figure 4.2: Frequency at generator 1 under different control methods.

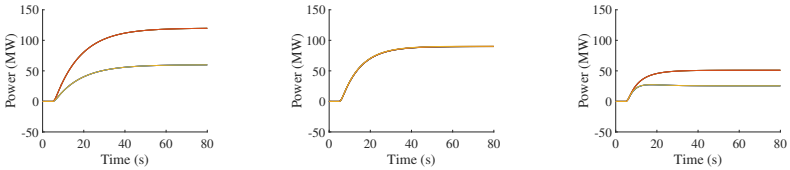

(a) DAI control (b) Decentralized pure integral control (c) Leaky integral control

Figure 4.3: Changes in active-power outputs of all the generators without noise.

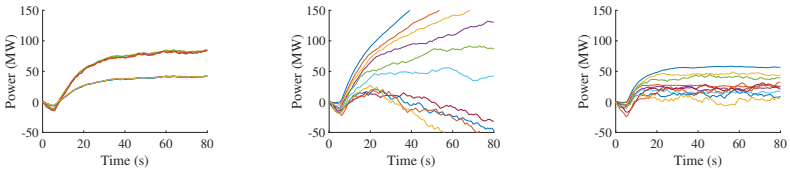

(a) DAI control (b) Decentralized pure integral control (c) Leaky integral control

Figure 4.4: Changes in active-power outputs of all the generators, under a frequency measurement noise bounded by $\overline{\eta} = 0.01$Hz.

ratio between G3, G5, G6, G9, G10 and other generators) as predicted in Corollary 4.2. However, leaky integral control solves the dispatch problem (4.21) thereby underestimating the net load compared to DAI which solves (4.4); see

Corollary 4.3. We conclude that fully decentralized leaky integral controller can achieve a performance similar to the communication-based DAI controller – though at the cost of steady-state offsets in both frequency and power adjustment.

4.5.2 COMPARISON BETWEEN CONTROLLERS WITH NOISE

Next, a noise term $\eta_i(t)$ is added to the frequency measurements ω in (4.34b), (4.7b), and (4.13b) for DAI, pure integral, and leaky integral control, respectively. The noise $\eta_i(t)$ is sampled from a uniform distribution on $[0, \overline{\eta}_i]$, with $\overline{\eta}_i$ selected such that the ratios of $\overline{\eta}_i$ between generators are $1:2:3:\cdots:10$ and $\|[\overline{\eta}_1, \overline{\eta}_2, \dots]\| = \overline{\eta} = 0.01$ Hz. The meaning of $\overline{\eta}$ here is consistent with that in Definition 4.1 and Theorem 4.3. At each generator i, the noise has non-zero mean $\overline{\eta}_i/2$ (inducing a constant measurement bias) and variance $\sigma^2_{\eta,i} = \overline{\eta}_i^2/12$.

Figure 4.2 (solid plots) shows the frequency at generator 1, and Figure 4.4 shows the changes in active-power outputs of all the generators under such a measurement noise. Observe from Figures 4.2(b)–4.2(c) and Figures 4.4(b)–4.4(c) that leaky integral control is more robust to measurement noise than pure integral control. Figures 4.4(a) and 4.4(c) show that the DAI control is even more robust than the leaky integral control in terms of generator power outputs, which is not surprising since the averaging process between neighbouring DAI controllers can effectively mitigate the effect of noise – thanks to communication.

4.5.3 IMPACTS OF LEAKY INTEGRAL CONTROL PARAMETERS

Next we investigate the impacts of inverse DC gains K_i and time constants T_i on the performance of leaky integral control.

First, we fix the integral time constant $T_i = \tau = 0.05$ s for every generator i, and tune the gains $K_i = k$ for generators G3, G5, G6, G9, G10; $K_i = 2k$ for other generators to ensure the same asymptotic power sharing as above. The following metrics of controller performance are calculated for the frequency at generator 1: (i) the steady-state frequency error without noise; (ii) the convergence time, which is defined as the time when frequency error enters and stays within $[0.95, 1.05]$ times its steady state; and (iii) the frequency root-mean-square-error (RMSE) from its nominal steady state, calculated over 60–80 seconds (the average RMSE over 100 random realizations is taken). The RMSE results from measurement noise $\eta_i(t)$ generated every second at every generator

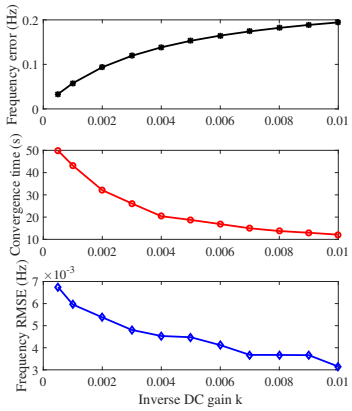

Figure 4.5: Steady-state error (upper), convergence time (middle), and RMSE (lower) of frequency at generator 1, as functions of the gain k for leaky integral control. The time constants are $T_i = \tau = 0.05\,\mathrm{s}$ for all generators.

i from a uniform distribution on $[-\overline{\eta}_i, \overline{\eta}_i]$, where the meaning of $\overline{\eta}_i$ is the same as in Section 4.5.2; $\eta_i(t)$ has zero mean so that the performance in mitigating steady-state bias and variance can be observed separately. Figure 4.5 shows these metrics as functions of k. It can be observed that the steady-state error increases with k, as predicted by Lemma 4.2; convergence is faster as k increases, in agreement with Theorem 4.2; and robustness to measurement noise is improved as k increases, as predicted by Theorem 4.3.

Next, we tune the integral time constants $T_i = \tau$ for all generators and fix $k = 0.005$, i.e., $K_i = 0.005$ for G3, G5, G6, G9, G10 and $K_i = 0.01$ for other generators, for a balance between steady-state and transient performance. Since the steady state is independent from τ, only the convergence time and RMSE of frequency at generator 1 are shown in Figure 4.6. It can be observed that convergence is faster as τ decreases, which is in line with Theorem 4.2. Robustness to measurement noise is improved as τ increases, which is in line with Theorem 4.3.

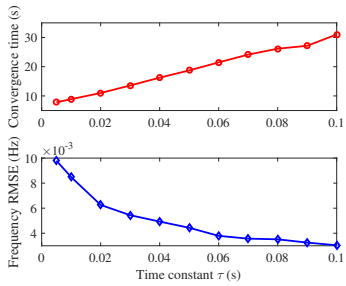

Figure 4.6: Convergence time (upper) and RMSE (lower) of frequency at generator 1, as functions of the time constant $T_i = \tau$ for leaky integral control. The gains K_i are 0.005 for G3, G5, G6, G9, G10 and 0.01 for other generators.

4.6 SUMMARY AND DISCUSSION

In the following, we summarize our findings and the various trade-offs that need to be taken into account for the tuning of the proposed leaky integral controller (4.13).

From the discussion following the Laplace-domain representation (4.14), the gains K_i and T_i of the leaky integral controller (4.13) can be understood as interpolation parameters for which the leaky integral controller reduces to a pure integrator ($K_i \searrow 0$) with gain T_i, a proportional (droop) controller ($T_i \searrow 0$) with gain K_i^{-1}, or no control action ($K_i, T_i \nearrow \infty$). Within these extreme parametrizations, we found the following trade-offs: The steady-state analysis in Section 4.4.1 showed that proportional power sharing and banded frequency regulation is achieved for any choice of gains $K_i > 0$: their sum gives a desired steady-state frequency performance (see Corollary 4.1), and their ratios give rise to the desired proportional power sharing (see Corollary (4.2)). However, a vanishingly small gain K_i is required for asymptotically exact frequency regulation (see Corollary 4.3), i.e., the case of integral control. Otherwise, the net load is always underestimated. With regards to stability, we inferred global stability for vanishing $K_i \searrow 0$ (see Theorem 4.1) but also an absence of robustness to measurement errors as in (4.12). On the other hand, for positive gains $K_i > 0$ we obtained nominal local exponential stability (see Theorem 4.2) with exponential rate as a function of K_i/T_i and robustness (in the form of exponential ISS with restrictions) to bounded measurement errors (see The-

orem 4.3) with increasing (respectively, non-decreasing) robustness margins to measurement noise as K_i (or T_i) become larger.

Our findings pose the question whether the leaky integral controller (4.13) actually improves upon proportional (droop) control (the case $T_i = 0$) with sufficiently large droop gain K_i^{-1}. The answers to this question can be found in practical advantages: (*i*) leaky integral control obviously low-pass filters measurement noise; (*ii*) has a finite bandwidth thus resulting in a less aggressive control action more suitable for slowly-ramping generators; and (*iii*) is not susceptible to wind-up (indeed, a proportional-integral control action with anti-windup reduces to a lag element (Franklin et al., 1994)). (*iv*) Other benefits that we did not touch upon in our analysis are related to classical loop shaping; e.g., the frequency for the phase shift can be specified for leaky integral control (4.13) to give a desired phase margin (and thus also practically relevant delay margin) where needed for robustness or overshoot.

In summary, our lag-element-inspired leaky integral control is fully decentralized, stabilizing, and can be tuned to achieve robust noise rejection, satisfactory steady-state regulation, and a desirable transient performance with exponential convergence. We showed that these objectives are not always aligned, and trade-offs have to be found. From a practical perspective, we recommend to tune the leaky integral controller towards robust steady-state regulation and to address transient performance with related lead-element-inspired controllers (Jiang et al., 2017).

4.7 TECHNICAL LEMMAS

We recall a technical lemma used in the main text.

Lemma 4.3 (Positivity of V)**.** *Suppose that Assumption 4.2 holds and that $B^\top \delta \in \Theta$. The Lyapunov function V specified in* (4.26) *satisfies*

$$\beta_1 \|x\|^2 \leq V(x) \leq \beta_2 \|x\|^2$$

for some positive constants β_1 and β_2, with x given in (4.24)*, provided that ε is sufficiently small.*

Proof. This proof follows the same line of arguments as the proof of Weitenberg et al. (2017a, Lemma 8), but accounts for our slightly different Lyapunov function. We will bound $V(x)$ in (4.26) term-by-term. The quadratic terms in

$\omega - \omega^*$ and $p - p^*$ are easily bounded in terms of the eigenvalues of the matrices M and T, respectively. The term in δ and δ^* is addressed in the second statement of Lemma 2.4. These three terms lead to the early bound

$$\begin{aligned}\min(\lambda_{\min}(M), \lambda_{\min}(T), \alpha_3)\|x\|^2 \leq\ & V(x)|_{\varepsilon=0} \\ & \leq \max(\lambda_{\max}(M), \lambda_{\max}(T), \alpha_4)\|x\|^2.\end{aligned}$$

The cross-term $\varepsilon(\nabla U(\delta) - \nabla U(\delta^*))^\top M\omega$ can be written as

$$\begin{pmatrix} \nabla U(\delta) - \nabla U(\delta^*) \\ \omega \end{pmatrix}^\top \begin{bmatrix} \mathbb{0} & \frac{\varepsilon}{2}M \\ \frac{\varepsilon}{2}M & \mathbb{0} \end{bmatrix} \begin{pmatrix} \nabla U(\delta) - \nabla U(\delta^*) \\ \omega \end{pmatrix}.$$

This allows us to apply Lemma 2.5, which yields

$$\begin{aligned}& - \|\nabla U(\delta) - \nabla U(\delta^*)\|^2 - \lambda_{\max}(M)^2\|\omega\|^2 \\ & \leq (\nabla U(\delta) - \nabla U(\delta^*))^\top M\omega \\ & \qquad \leq \|\nabla U(\delta) - \nabla U(\delta^*)\|^2 + \lambda_{\max}(M)^2\|\omega\|^2.\end{aligned}$$

By applying the first statement of Lemma 2.4, we can bound the entire Lyapunov function using

$$\begin{aligned}\beta_1 &= \min(\lambda_{\min}(M) - \varepsilon\lambda_{\max}(M)^2, \lambda_{\min}(T), \alpha_3 - \varepsilon\alpha_2^2) \\ \beta_2 &= \max(\lambda_{\max}(M) + \varepsilon\lambda_{\max}(M)^2, \lambda_{\max}(T), \alpha_4 + \varepsilon\alpha_2^2).\end{aligned}$$

Finally, we select ε sufficiently small so that $\beta_1 > 0$. □

PART II

Consensus algorithms for DC microgrids

Introduction

In this part, we exchange the AC power grid for the DC microgrid.

Many energy sources, storage devices and appliances intrinsically operate using direct current. This stimulates interest in the design and use of DC microgrids, which have the additional desirable feature of preventing the use of inefficient power conversions at different stages. Such grids are already in use in some small-scale grids e.g. on ships, planes and trains. In addition, if power is generated far away from its consumers, e.g. in wind farms at sea, it should be transported to the consumption sites with low losses. High Voltage Direct Current (HVDC) networks perform comparatively better at this than AC networks.

Given these developments, the need arises for a deeper understanding of stability and control of these dynamical networks. In this part, we propose and analyse control algorithms for DC microgrids, that aim for economic optimality by enforcing power sharing among the different power sources.

Below, we give a short survey of previous approaches to control of DC power networks. Conventionally, secondary control adjusts the set point for a local proportional (droop) controller. Zhao and Dörfler (2015) complement this approach with a consensus control algorithm, preventing voltage drift and achieving optimal current injection. A similar approach is found by Tucci et al. (2016), allowing additionally for 'Plug-and-Play' addition and removal of generators. Nasirian et al. (2015) replace the secondary control instead by a separate voltage and current regulator, and Belk et al. (2016) use the Brayton-Moser formalism to show that voltage regulation can be achieved by decentralized integral control. Moayedi and Davoudi (2016) propose a distributed control method for enforcing power sharing among a cluster of DC microgrids, but provide no formal analysis.

Various auxiliary challenges have been considered as well. Meng et al. (2016) study the interaction between the communication network and the physical network which occurs in consensus-like control methods, and their effects on stability of the microgrid. The feasibility of the nonlinear algebraic equations in DC power circuits is studied by Barabanov et al. (2016); Simpson-Porco et al.

(2015); Lavei et al. (2011).

Finally, several works have focused on the particular research area of HVDC transmission systems. Sarlette et al. (2012) focuses on frequency control in HVDC grids connecting multiple AC power networks. Andreasson et al. (2014c) study a distributed control strategy that keeps the voltages close to a nominal value and guarantees fair power sharing are considered. Zonetti et al. (2015) exploit a port-Hamiltonian framework to show that HVDC networks can be asymptotically stabilized using decentralized PI controllers. Zonetti et al. (2016) study existence of equilibria and power sharing under decentralized droop control. We refer to Zonetti (2016, Chapter 4) for an extensive bibliography of HVDC transmission systems.

CONTRIBUTIONS

In this part, we aim to provide control algorithms that exhibit the following features.

Power sharing, i.e. the power sources provide power in prescribed ratios for a wide range of load magnitudes,

Voltage regulation, i.e. all voltages remain within a compact set around the nominal voltage.

In addition, we allow for various kinds and combinations of loads, referred to hereafter as ZIP loads, which stands for constant impedance, constant current and constant power loads respectively. We will also encounter ZI loads, which are ZIP loads without the constant power load component.

Power sharing is an important feature in microgrid control algorithms. It forces all generation units to generate a portion of the power required by the loads in the network. Absent this feature, certain load configurations can force a small set of generators to provide a disproportionate amount of the power required by the network, which might lead to them exceeding their capacity limits.

Proportional (droop) controllers are traditionally used for microgrid control. They strike a trade-off between power sharing and voltage control, and therefore require careful tuning given the load ranges to regulate the voltages and power generation to safe levels. The controllers proposed in this part do not have this limitation, and are thus an improvement upon droop control. This is enabled by assuming the presence of a communication network between the generators, which allows the exchange of various measurements.

OUTLINE

CHAPTER 5

In this chapter, we restrict ourselves to DC networks with resistive transmission lines. In this setting, we propose a distributed control algorithm, enabled by communicating power measurements among the source nodes using a communication network. The controllers set the source voltages such that the power provided by each power source becomes proportional to a user-configurable weight distribution. Additionally, the weighted geometric average of source voltages is preserved.

To analyse the system of non-linear DAE resulting from the controller, network and ZIP loads, we use Lyapunov arguments. Our Lyapunov function of choice is constructed from the power dissipated in the network, together with various terms to take into account the specific dynamics of the system. In an interesting development, we then see that the system can be written as a weighted gradient of the Lyapunov function, which is crucial to the stability analysis. Moreover, the voltage excursion can be bounded using the sub-level sets of the Lyapunov function, combined with the aforementioned conservation of the geometric average of the source voltages.

CHAPTER 6

This Chapter provides an extension to the previous Chapter to power networks with resistive-inductive (RL) power lines. In this extension, we omit the constant power loads discussed previously, and focus on networks with ZI-loads. Again, we propose a distributed control algorithm, in which the power sources employ a communication network to exchange current flow measurements. These new controllers are able to regulate the power injected by each source to the average power injected by the sources. In addition, the geometric average of the voltages at the sources is preserved.

Using a slightly modified version of the Lyapunov function from Chapter 5, the system can once more be viewed as a weighted gradient system. This allows to show convergence of the power injected by the sources, and boundedness of the voltages at the sources.